

## Novel Dirhodium Coordination Polymers: The Impact of Side Chains on Cyclopropanation

Jiquan Liu,<sup>[a,b]</sup> Yeping Xu,<sup>[b]</sup> Pedro B. Groszewicz,<sup>[b]</sup> Martin Brodrecht,<sup>[b]</sup> Claudia Fasel,<sup>[c]</sup>  
Kathrin Hofmann,<sup>[b]</sup> Xijuan Tan,<sup>[d]</sup> Torsten Gutmann<sup>[b]\*</sup> and Gerd Buntkowsky<sup>[b]\*</sup>

<sup>a</sup> *Key Laboratory of Synthetic and Natural Functional Molecule Chemistry, College of Chemistry and Materials Science, Northwest University, 710127 Xi'an, P. R. China*

<sup>b</sup> *Eduard-Zintl-Institute for Inorganic Chemistry and Physical Chemistry, Technical University Darmstadt, Alarich-Weiss-Straße 8, 64287 Darmstadt, Germany*

<sup>c</sup> *FB Material- und Geowissenschaften, Technical University Darmstadt, Alarich-Weiss-Straße 2, 64287 Darmstadt, Germany*

<sup>d</sup> *Laboratory of Mineralization and Dynamics, College of Earth Sciences and Land Resources, Chang'an University, 710054 Xi'an, P. R. China*

E-mail: [gutmann@chemie.tu-darmstadt.de](mailto:gutmann@chemie.tu-darmstadt.de)

[Gerd.Buntkowsky@chemie.tu-darmstadt.de](mailto:Gerd.Buntkowsky@chemie.tu-darmstadt.de)

### Content

1. ATR-FTIR of synthesized ditopic ligands .....	2
2. Solution-state NMR of synthesized ditopic ligands .....	3
3. TG-DTA analyses .....	5
4. SEM and XRD .....	8
5. UV-vis spectroscopy .....	10
6. XPS .....	12
7. Leaching test .....	13
8. Calculation of turnover frequency (TOF).....	15
9. References .....	16

## 1. ATR-FTIR of synthesized ditopic ligands

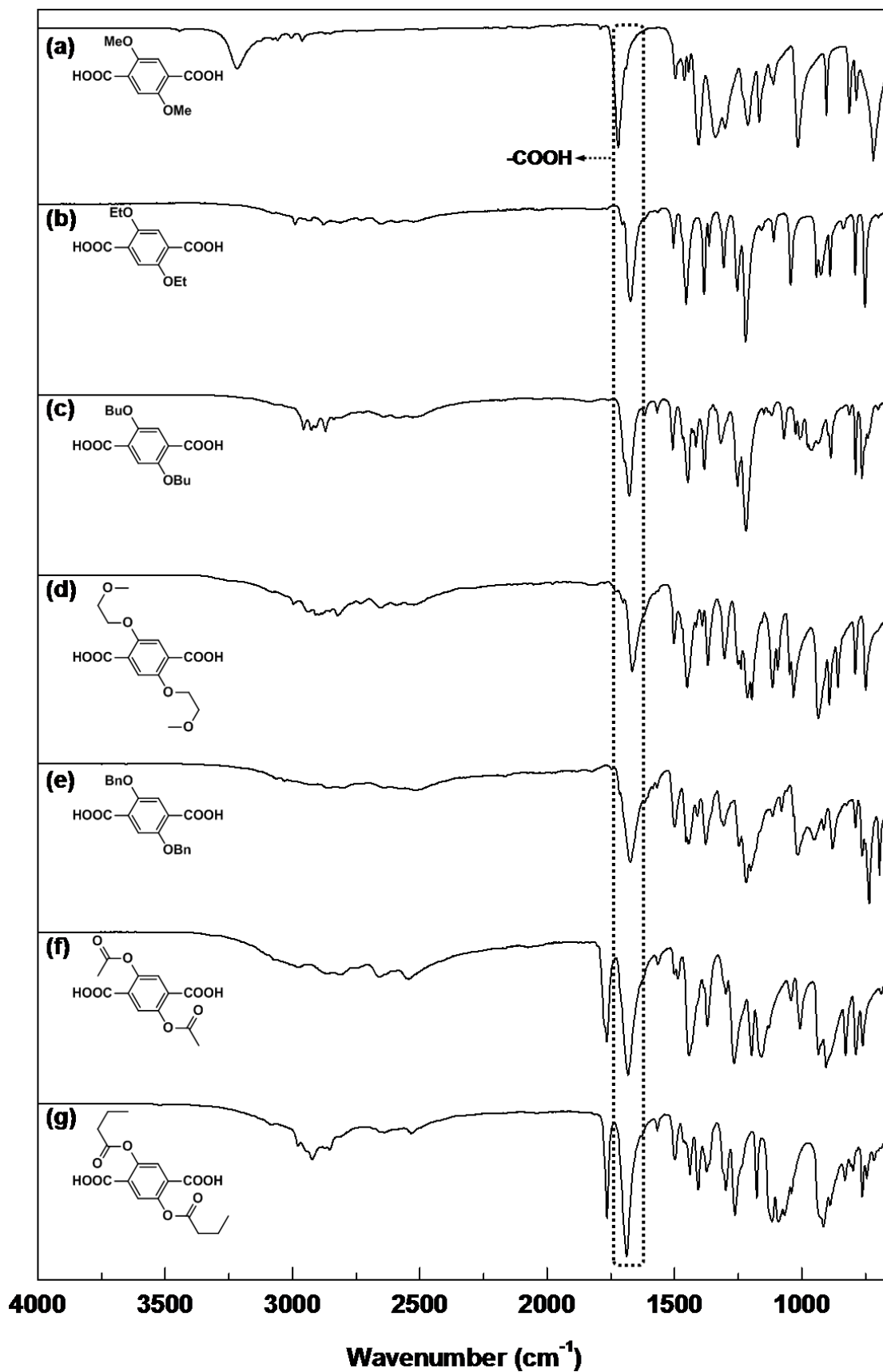


**Figure S1.** ATR-FTIR of H<sub>2</sub>L1(a), H<sub>2</sub>L2(b), H<sub>2</sub>L3(c), H<sub>2</sub>L4(d), H<sub>2</sub>L5(e), H<sub>2</sub>L6(f) and H<sub>2</sub>L7(g).

## 2. Solution-state NMR of synthesized ditopic ligands

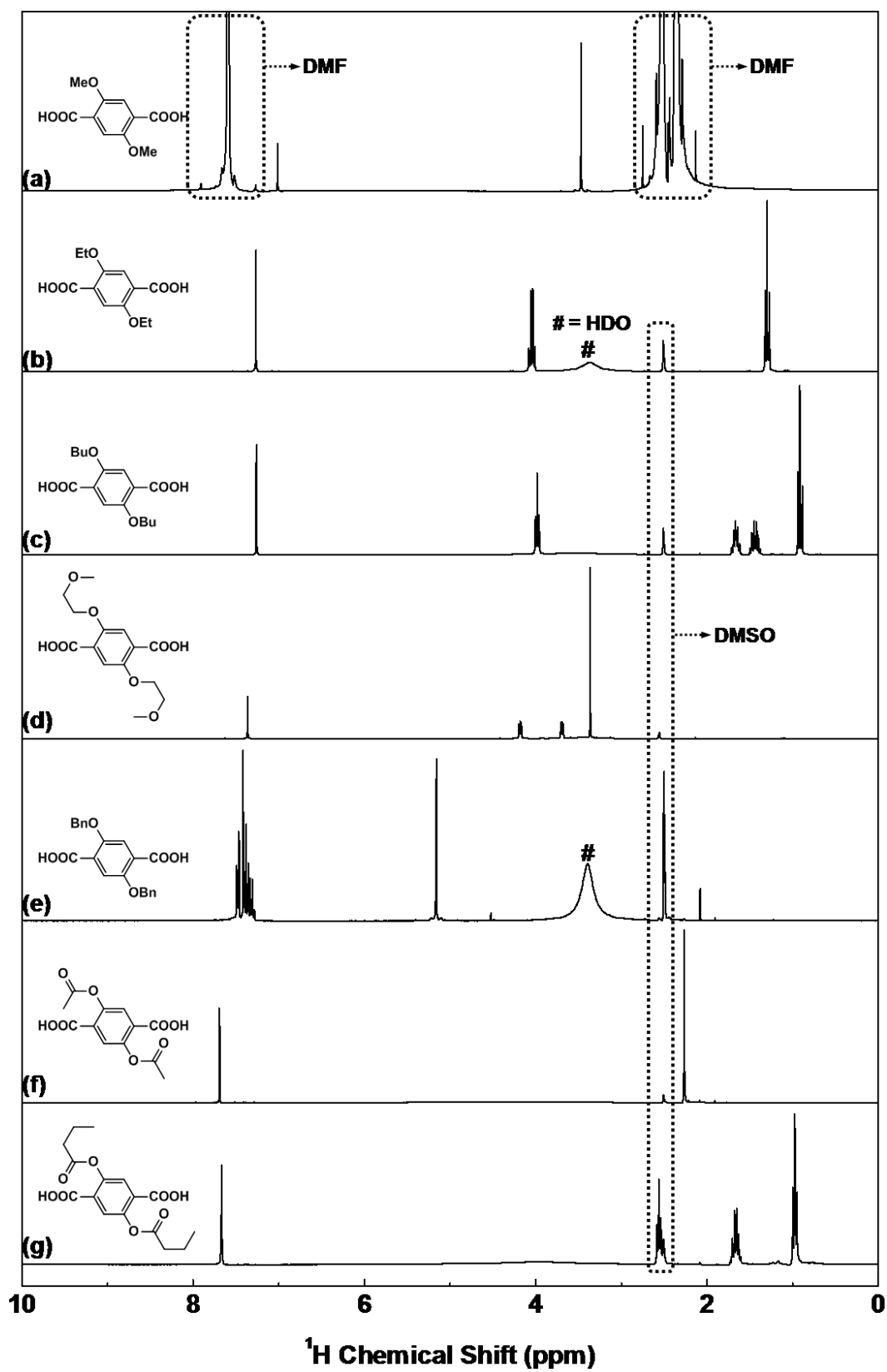


**Figure S2.**  $^1\text{H}$  solution-state NMR of H<sub>2</sub>L1(a), H<sub>2</sub>L2(b), H<sub>2</sub>L3(c), H<sub>2</sub>L4(d), H<sub>2</sub>L5(e), H<sub>2</sub>L6(f) and H<sub>2</sub>L7(g).

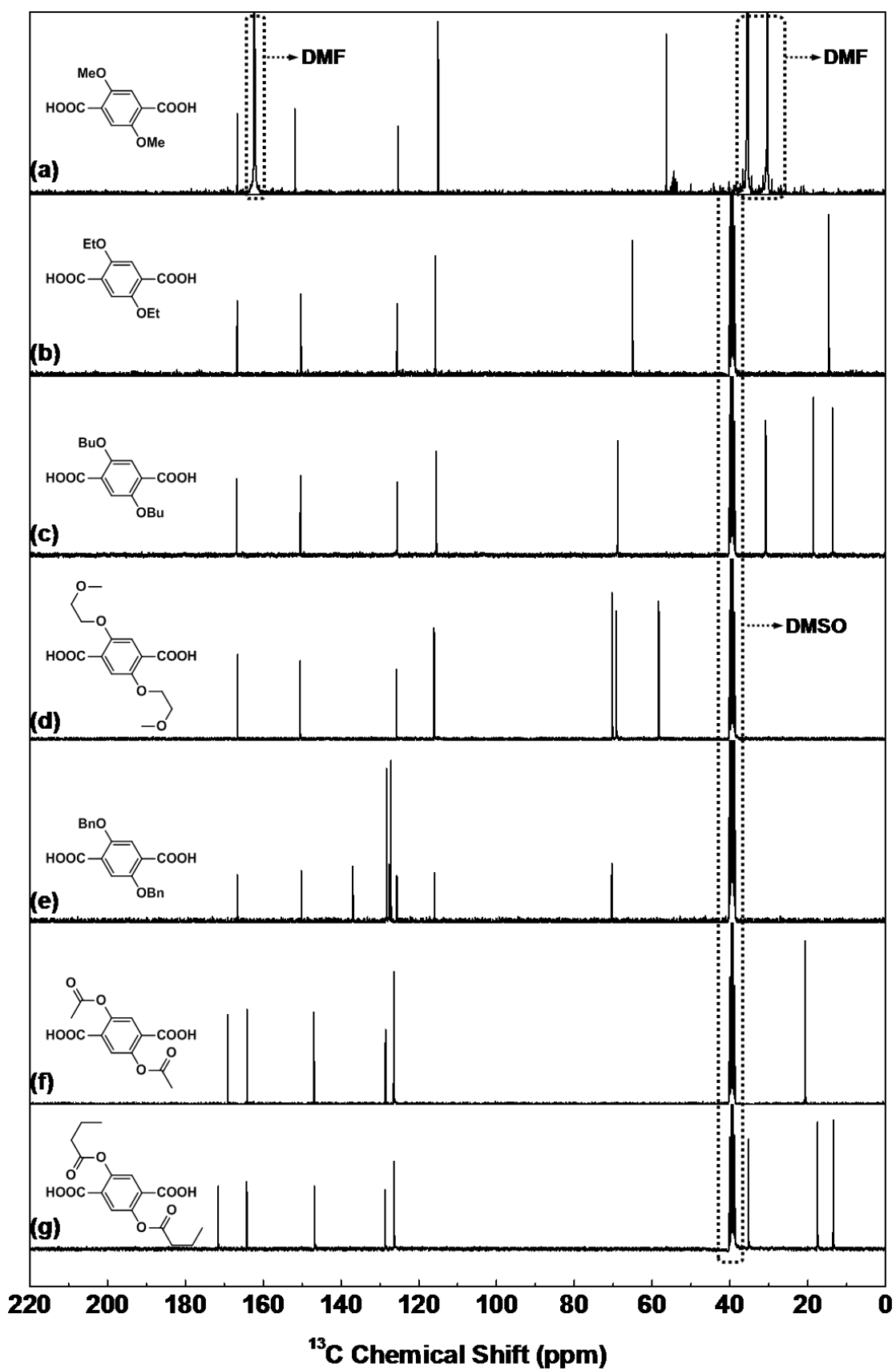


**Figure S3.**  $^{13}\text{C}$  solution-state NMR of H<sub>2</sub>L1(a), H<sub>2</sub>L2(b), H<sub>2</sub>L3(c), H<sub>2</sub>L4(d), H<sub>2</sub>L5(e), H<sub>2</sub>L6(f) and H<sub>2</sub>L7(g). Note: H<sub>2</sub>L1 was dissolved in DMF with 1–2 drops of D<sub>2</sub>O, while H<sub>2</sub>L<sub>n</sub> (n = 2–7) were dissolved in DMSO-d<sub>6</sub>.

### Experimental Details:

$^1\text{H}$  and  $^{13}\text{C}$  solution-state NMR spectra were recorded on a 7 T Bruker Avance II 300 spectrometer corresponding to frequencies of 299.91 MHz for  $^1\text{H}$  and 75.41 MHz for  $^{13}\text{C}$ . Typically,  $^1\text{H}$  spectra were recorded with single pulse excitation employing a  $30^\circ$  excitation pulse of ca. 4.4  $\mu\text{s}$ , a relaxation delay of 1 s and 32-64 scans.  $^{13}\text{C}$  spectra were recorded with single pulse excitation employing a  $30^\circ$  excitation pulse of ca. 3.1  $\mu\text{s}$ , a relaxation delay of 0.5 s and 600-1500 scans. Protons were decoupled during data acquisition employing the waltz16 [1] sequence.

### 3. TG-DTA analyses

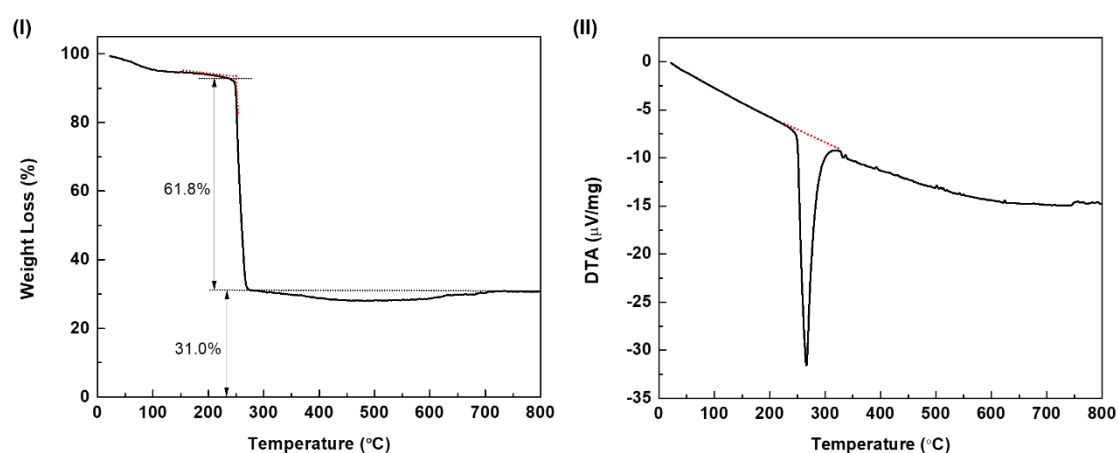


**Figure S4.** TG curve (I) and DTA curve (II) of  $\text{Rh}_2\text{-L1}$  under  $\text{O}_2$  atmosphere.

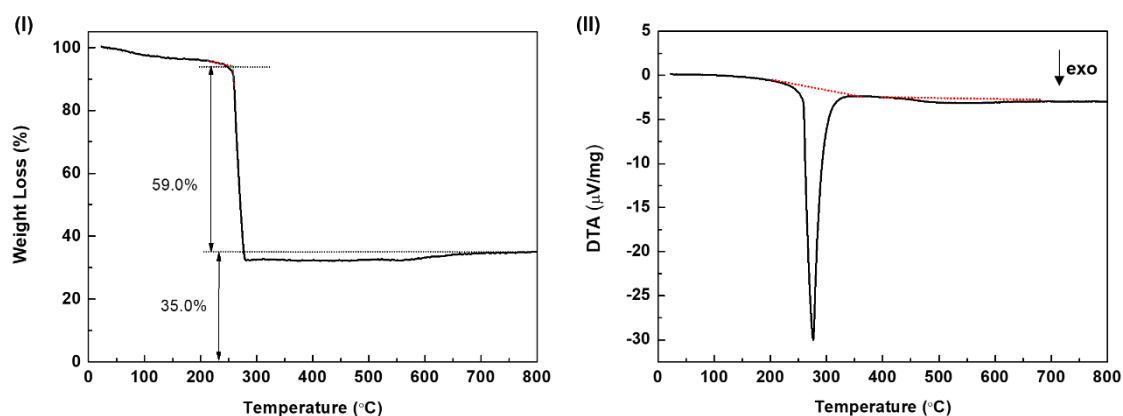


**Figure S5.** TG curve (I) and DTA curve (II) of  $\text{Rh}_2\text{-L2}$  under  $\text{O}_2$  atmosphere.

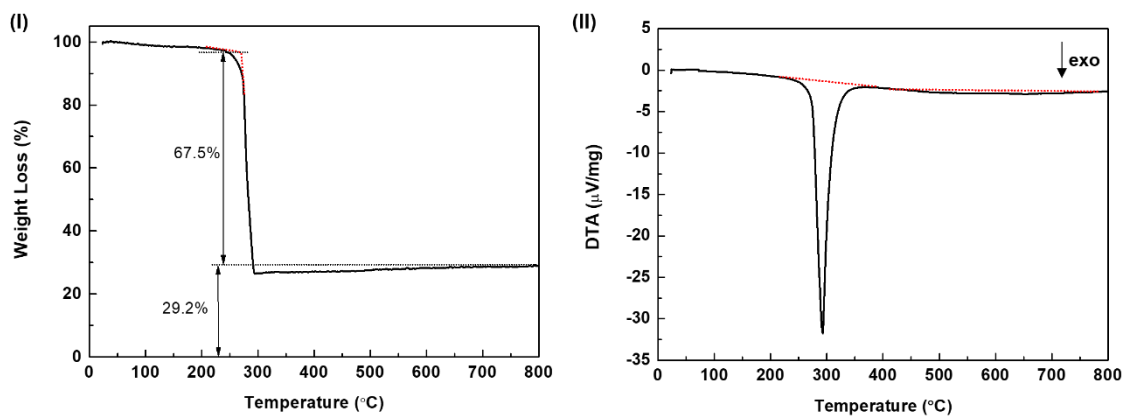


**Figure S6.** TG curve (I) and DTA curve (II) of Rh<sub>2</sub>-L3 under O<sub>2</sub> atmosphere.

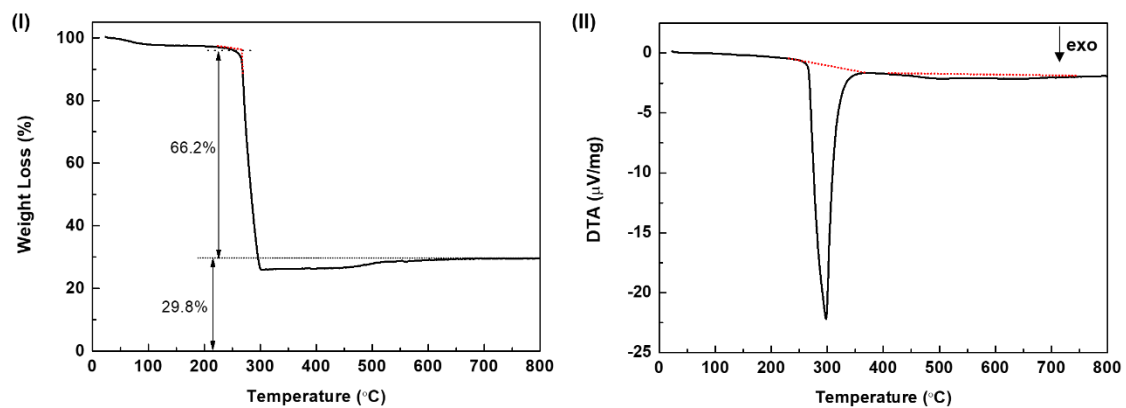


**Figure S7.** TG curve (I) and DTA curve (II) of Rh<sub>2</sub>-L4 under O<sub>2</sub> atmosphere.

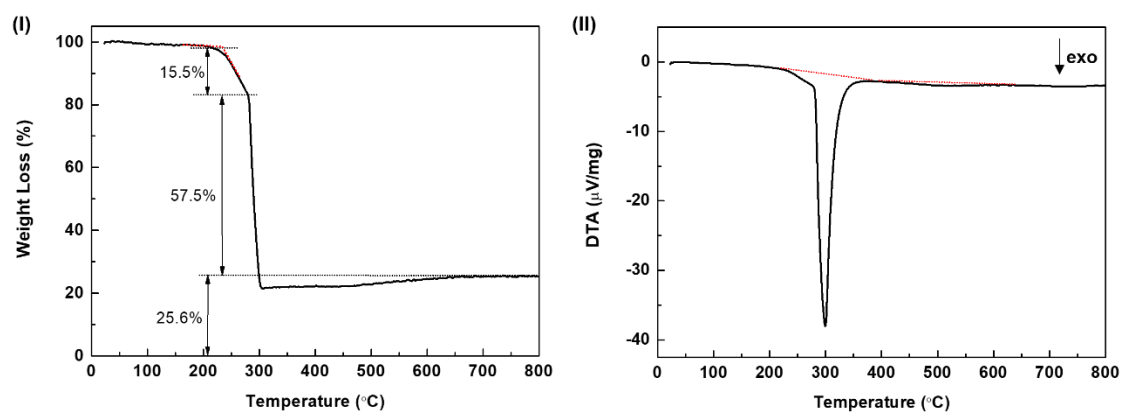


**Figure S8.** TG curve (I) and DTA curve (II) of Rh<sub>2</sub>-L5 under O<sub>2</sub> atmosphere.

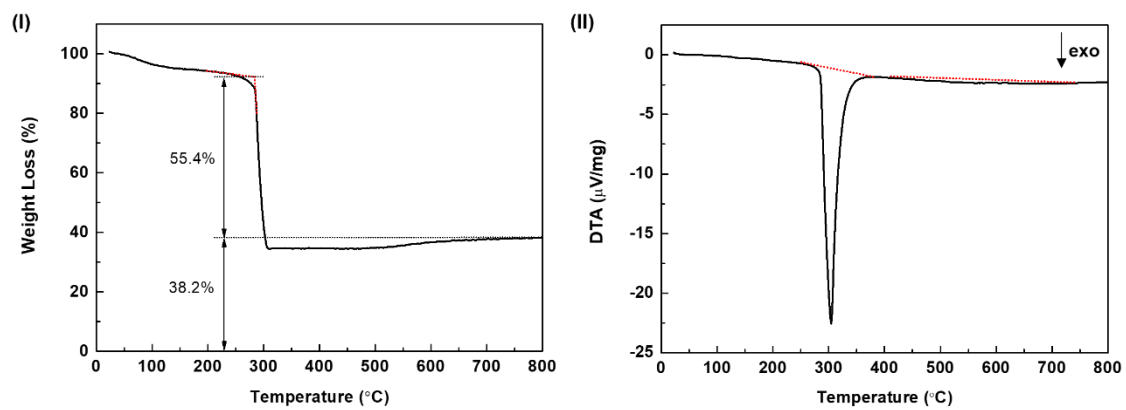


**Figure S9.** TG curve (I) and DTA curve (II) of Rh<sub>2</sub>-L6 under O<sub>2</sub> atmosphere.

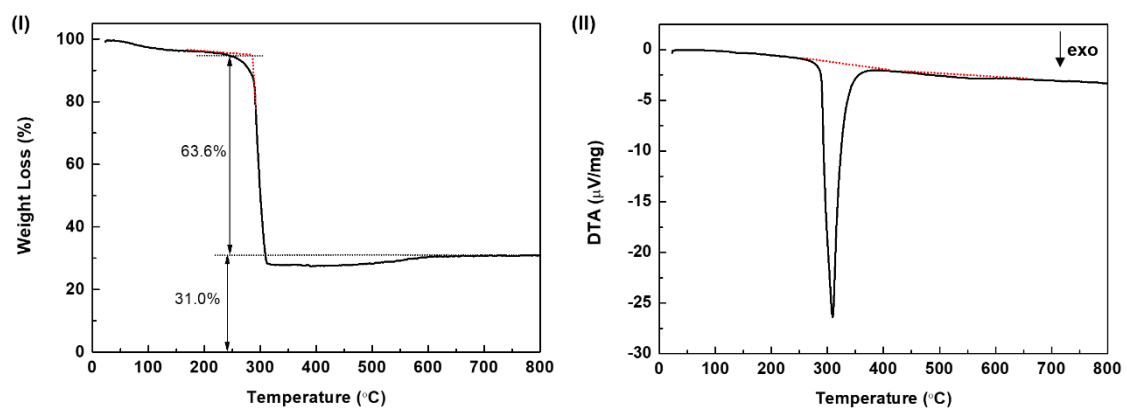


**Figure S10.** TG curve (I) and DTA curve (II) of Rh<sub>2</sub>-L7 under O<sub>2</sub> atmosphere.

#### 4. SEM and XRD

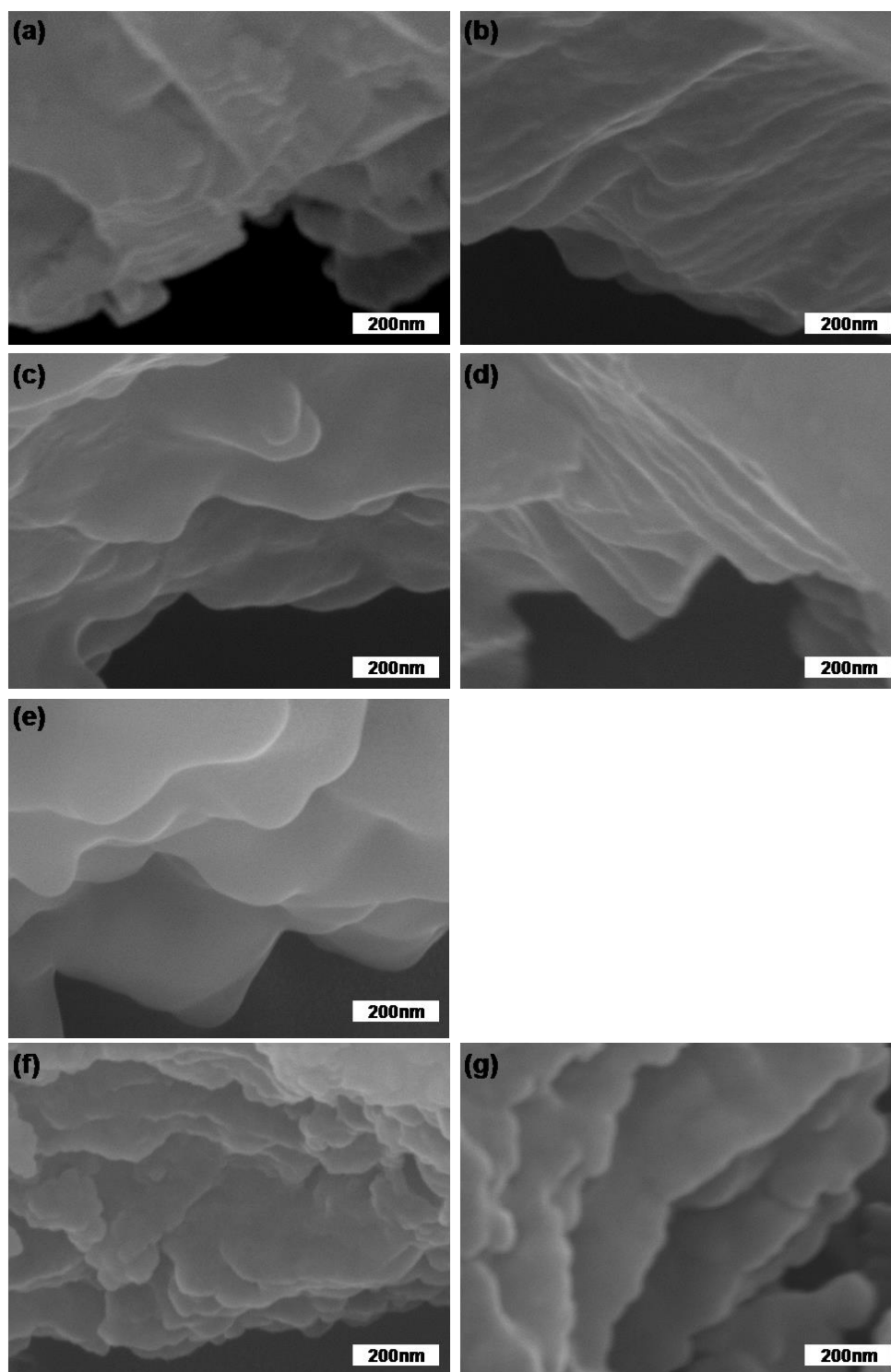


**Figure S11.** SEM of Rh<sub>2</sub>-L1(a), Rh<sub>2</sub>-L2(b), Rh<sub>2</sub>-L3(c), Rh<sub>2</sub>-L4(d), Rh<sub>2</sub>-L5(e), Rh<sub>2</sub>-L6(f) and Rh<sub>2</sub>-L7(g).



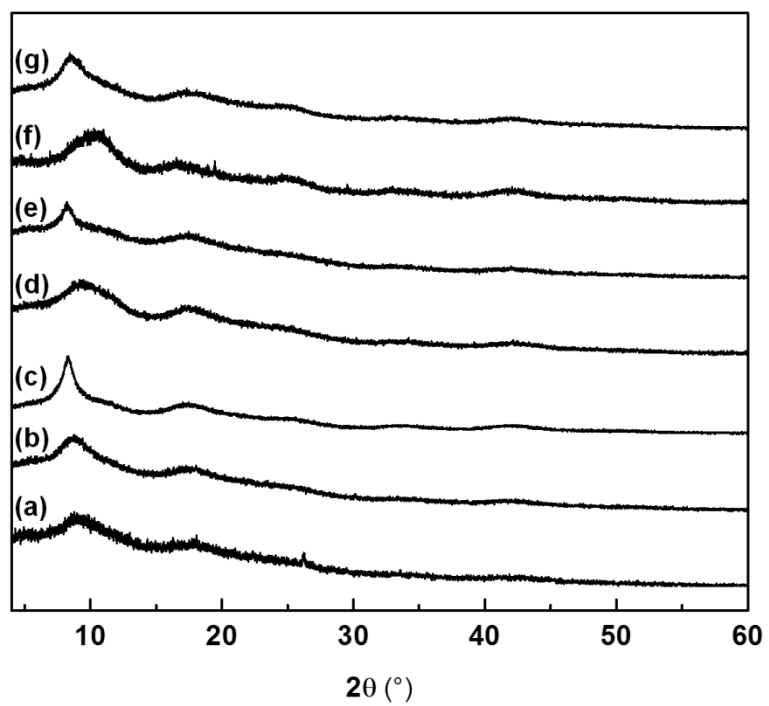


**Figure S12.** XRD patterns of Rh<sub>2</sub>-L1(a), Rh<sub>2</sub>-L2(b), Rh<sub>2</sub>-L3(c), Rh<sub>2</sub>-L4(d), Rh<sub>2</sub>-L5(e), Rh<sub>2</sub>-L6(f) and Rh<sub>2</sub>-L7(g).

## 5. UV-vis spectroscopy

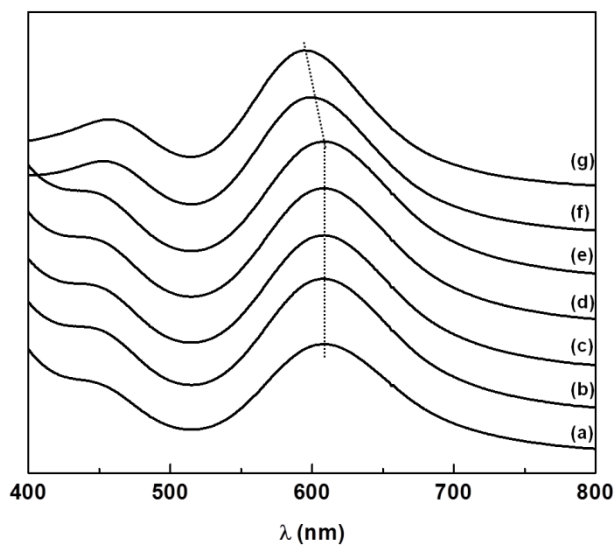


**Figure S13.** UV-vis spectrum of  $\text{Rh}_2(\text{TFA})_4$   $\text{CH}_2\text{Cl}_2$  solution by adding ethyl ether (EtOEt) probe molecule with  $\text{Rh}_2(\text{TFA})_4/\text{EtOEt}$  molar ratio of 1/0 (a), 1/1 (b), 1/2 (c), 1/6 (d), 1/10 (e), 1/1800 (f) and 1/3600 (g).

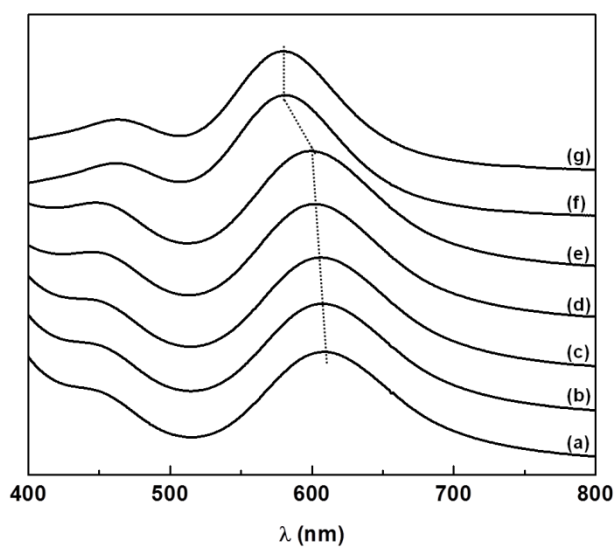


**Figure S14.** UV-vis spectrum of  $\text{Rh}_2(\text{TFA})_4$   $\text{CH}_2\text{Cl}_2$  solution by adding ethanol (EtOH) probe molecule with  $\text{Rh}_2(\text{TFA})_4/\text{EtOH}$  molar ratio of 1/0 (a), 1/1 (b), 1/2 (c), 1/6 (d), 1/10 (e), 1/1800 (f) and 1/3600 (g).

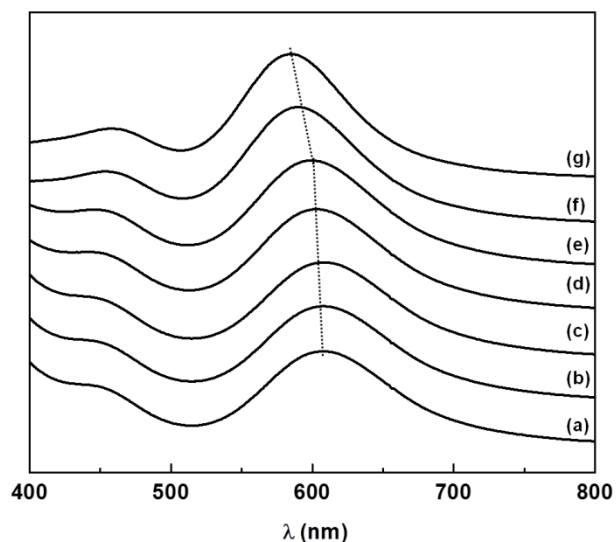


**Figure S15.** UV-vis spectrum of  $\text{Rh}_2(\text{TFA})_4$   $\text{CH}_2\text{Cl}_2$  solution by adding acetone probe molecule with  $\text{Rh}_2(\text{TFA})_4/\text{acetone}$  molar ratio of 1/0 (a), 1/1 (b), 1/2 (c), 1/6 (d), 1/10 (e), 1/1800 (f) and 1/3600 (g).

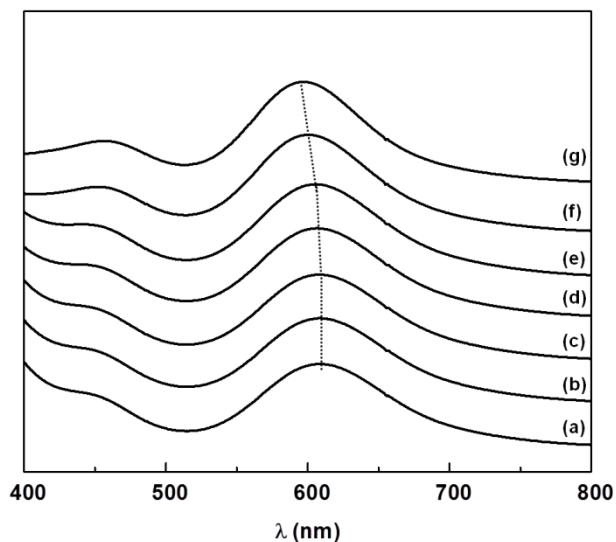


**Figure S16.** UV-vis spectrum of  $\text{Rh}_2(\text{TFA})_4$   $\text{CH}_2\text{Cl}_2$  solution by adding ethyl acetate (EtOAc) probe molecule with  $\text{Rh}_2(\text{TFA})_4/\text{EtOAc}$  molar ratio of 1/0 (a), 1/1 (b), 1/2 (c), 1/6 (d), 1/10 (e), 1/1800 (f) and 1/3600 (g). Note: These spectra were reproduced from our previous work (see ref <sup>[2]</sup>).

*Experiment details:*

The solution was prepared by dissolving 0.0155 g (23.5  $\mu\text{mol}$ ) of  $\text{Rh}_2(\text{TFA})_4$  into 25 mL  $\text{CH}_2\text{Cl}_2$  resulting in a concentration of 0.94  $\text{mmol}\cdot\text{L}^{-1}$ . All liquid samples were recorded on a TIDAS 100 MCS spectrometer (J&M Analytik AG). For each measurement, 0.6 mL solution was added into ca. 1 mL quartz cuvette (10.00 mm QS Hellma Analytics).

## 6. XPS

The compositions of obtained dirhodium coordination polymers can be reflected via wide scan X-ray photoelectron spectra (ESI Figure S17). The electron binding energies obtained at 531 eV (O1s), 522 eV (Rh3p<sub>1/2</sub>), 497 eV (Rh3p<sub>3/2</sub>), 312-308 eV (Rh3d<sub>3/2</sub> and Rh3d<sub>5/2</sub>) and 284 eV (C1s) reflect the main composition of dirhodium coordination polymers.<sup>[3]</sup> The appearance of an electron binding energy at 688 eV, assigns to F1s which underlines the occurrence of trifluoroacetate residues in the obtained dirhodium coordination polymers.<sup>[3a]</sup> This observation further supports the incomplete ligand exchange as suggested by the <sup>13</sup>C CP MAS NMR (Figure 2 in main text) and <sup>19</sup>F MAS NMR spectra (Figure 3 in main text).

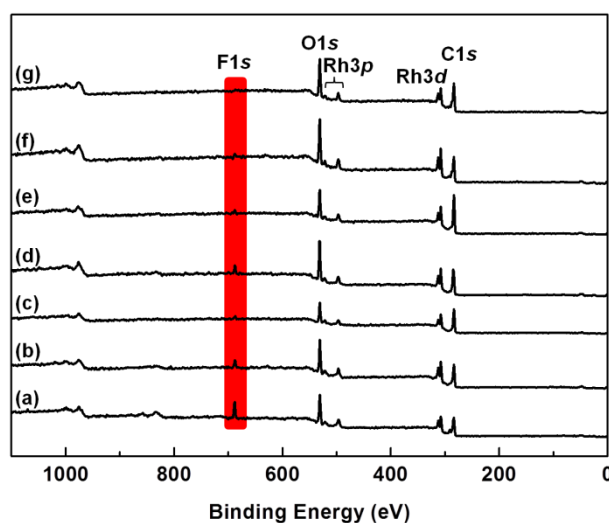


**Figure S17.** XPS of dirhodium coordination polymers in wide scan mode, Rh<sub>2</sub>-L1(a), Rh<sub>2</sub>-L2(b), Rh<sub>2</sub>-L3(c), Rh<sub>2</sub>-L4(d), Rh<sub>2</sub>-L5(e), Rh<sub>2</sub>-L6(f) and Rh<sub>2</sub>-L7(g).

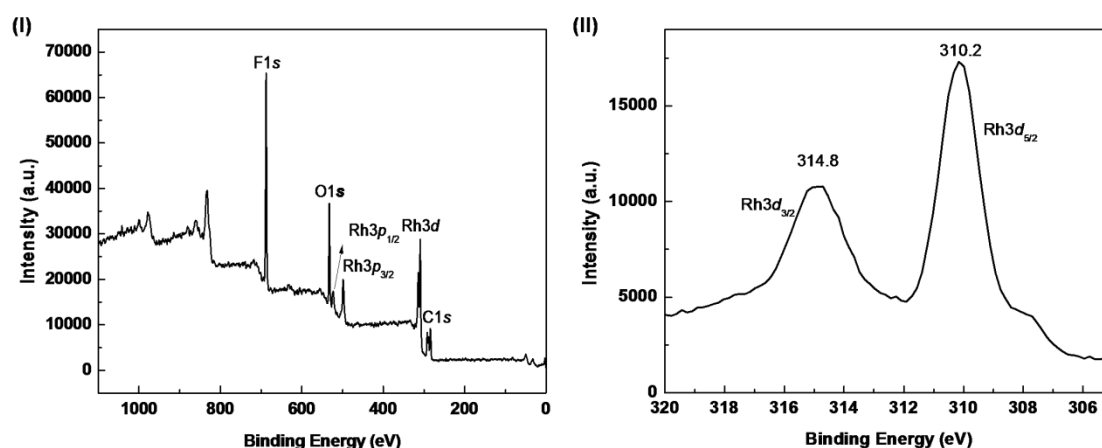


**Figure S18.** XPS of Rh<sub>2</sub>(TFA)<sub>4</sub> in (I) wide scan mode and (II) high resolution mode. Note: The figure was reproduced from our previous work (see electronic supporting information of ref.<sup>[2]</sup>)

## 7. Leaching test

To prove the heterogeneous nature of the dirhodium coordination polymers, Rh<sub>2</sub>-L2 was chosen for a case study (ESI Figure S19). The catalyst Rh<sub>2</sub>-L2 was filtrated at 15 min and the product yields in the filtered solution stayed around 35% along the reaction time until 120 min, even for extended reaction time (240 min). Furthermore, the filtrated reaction medium was collected for ICP-MS measurement to determine the rhodium contain. As can be seen in Table S1, the rhodium fraction was found to be ca. 160 ppb. Similar to our previous work,<sup>[2]</sup> both chemical confinement and separation of binding sites from the catalytic sites (Figure S19b) seem to be responsible for the negligible release of active sites during the cyclopropanation.

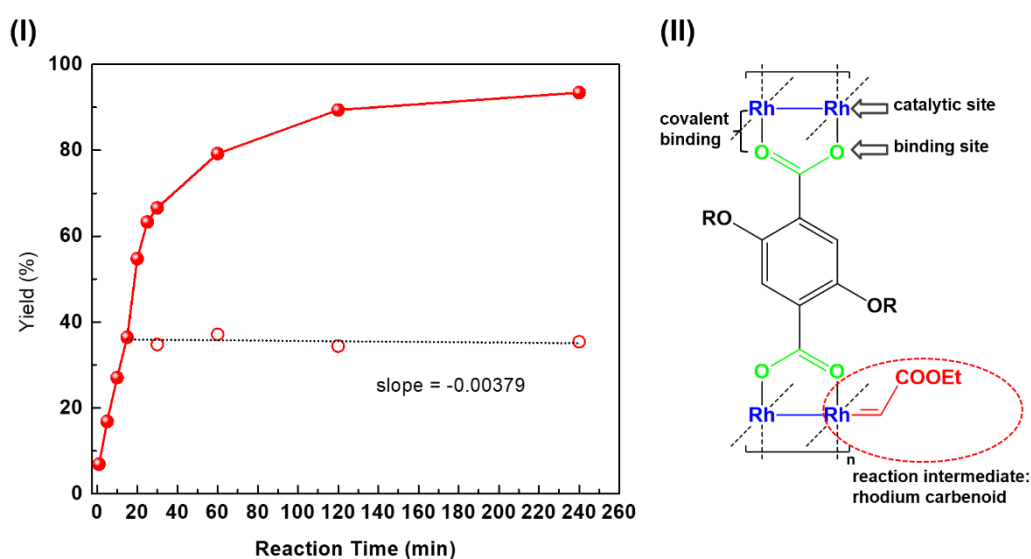


**Figure S19** (I) Leaching test: reaction in the presence of Rh<sub>2</sub>-L2 (b) and after removal of Rh<sub>2</sub>-L2 (b'), and (II) schematic representation of binding site and catalytic site in dirhodium coordination polymers.

### Testing Report

Client Name	Liu Jiquan	Report No.	ICPMS-JC-20180708			
Number of Samples	2	Testing date	2018/7/8			
Unit	ppb	Instrument	ThermoFisher Scientific X series ICP-MS			
Analytical Center	The Laboratory of Mineralization and Dynamics, Chang'an University					
Testing element	Analytical No.		Sample No.			
	JQQ-b-1	LJQ-b-2				
	Rh <sub>2</sub> -L2	Rh <sub>2</sub> -L2				
Rh	160.5	161.8				

**Table S1** The rhodium fraction in the reaction medium as determined by ICP-MS.

### *Experiment details*

The Rhodium content was determined by a Thermofisher Scientific X series ICP-MS instrument (Waltham, MA, USA) in the Laboratory of Mineralization and Dynamics, Chang'an University. After removal of the Rh<sub>2</sub>-L2 catalyst via centrifugation, the clear solution was collected and the solvent was removed at elevated temperature (50-100 °C). The residue was further treated at 500 °C under air for 6 h. After burning the organic species, the sample was shifted into a Teflon vessel, and 1.0 mL of concentrated HNO<sub>3</sub> (68% v/v, AR grade) was added. After continually heating at 130 °C for 2 h, the solution was evaporated until incipient dryness. Thereafter, the samples were diluted using 2% HNO<sub>3</sub> (v/v) to 13.0 mL calibrated mark. With the solutions filtrated through the filter paper (0.22 μm), the Rh levels were directly quantified by ICP-MS.

## 8. Calculation of turnover frequency (TOF)

The TOFs were calculated from the yield according to ref.<sup>[4]</sup> employing the following equation:

$$\text{TOF} = n_{(\text{EDA})} * \text{yield} / n_{(\text{catalyst, exp})} / t ,$$

where t is the reaction time,  $n_{(\text{EDA})}$  is the amount of EDA (0.5 mmol) and  $n_{(\text{catalyst, exp})}$  is the amount of dirhodium units calculated from the nominal concentration of the weighted samples,  $n_{(\text{catalyst, nom})}$ , which is ca. 9.3  $\mu\text{mol}$  for all coordination polymers, multiplied by the ratio of the nominal concentration (Rh%(nominal)) calculated for perfect stoichiometric exchange to the experimental Rh<sub>2</sub> concentration from TGA (Rh%(TGA) ):

$$n_{(\text{catalyst, exp})} = n_{(\text{catalyst, nom})} * (\text{Rh}(\%(\text{nominal})) / \text{Rh}(\%(\text{TGA}))) .$$

**Table S1.** Calculation of the TOF for each catalyst at each time point.

t (min)	Rh <sub>2</sub> -L1		Rh <sub>2</sub> -L2		Rh <sub>2</sub> -L3		Rh <sub>2</sub> -L4		Rh <sub>2</sub> -L5		Rh <sub>2</sub> -L6		Rh <sub>2</sub> -L7	
	yield (%)	TOF (h <sup>-1</sup> )	yield (%)	TOF (h <sup>-1</sup> )	yield (%)	TOF (h <sup>-1</sup> )	yield (%)	TOF (h <sup>-1</sup> )	yield (%)	TOF (h <sup>-1</sup> )	yield (%)	TOF (h <sup>-1</sup> )	Yield (%)	TOF (h <sup>-1</sup> )
1	0.9	35.5	5.4	176.9	2.4	82.7	0.0	0.0	3.1	109.1	4.9	136.0	0.0	0.0
2.5	1.3	20.8	8.4	110.1	4.0	54.1	0.0	0.0	3.4	48.0	7.5	84.1	0.5	5.4
5	1.9	15.5	12.1	79.5	7.6	51.4	0.0	0.0	4.1	28.8	10.3	57.8	0.5	2.7
7.5	2.2	12.0	14.8	65.0	11.9	53.8	0.0	0.0	4.5	21.2	13.1	49.0	0.6	2.3
10	2.6	10.7	20.4	67.0	16.6	56.3	0.0	0.0	5.4	19.0	14.9	41.8	0.5	1.6
15	3.6	9.6	32.8	72.0	22.3	50.3	0.0	0.0	6.2	14.6	16.9	31.6	0.8	1.7
20	3.7	7.5	49.6	81.8	28.9	49.0	0.0	0.0	7.3	12.8	18.7	26.2	1.0	1.5
25	3.9	6.3	54.7	72.1	35.9	48.6	1.2	1.6	7.9	11.1	21.4	23.9	0.9	1.1
30	4.2	5.6	62.4	68.5	41.0	46.4	1.3	1.4	9.4	11.0	21.7	20.3	1.3	1.3
60	7.3	4.9	89.3	49.0	61.4	34.7	2.3	1.3	20.7	12.2	27.7	12.9	2.9	1.5
120	10.5	3.5	91.1	25.0	75.7	21.4	10.1	2.8	26.8	7.9	35.2	8.2	7.9	2.0

## 9. References

- [1] aA. J. Shaka, J. Keeler, R. Freeman, *Journal of Magnetic Resonance* **1983**, *53*, 313-340; bA. J. Shaka, J. Keeler, T. Frenkiel, R. Freeman, *Journal of Magnetic Resonance* **1983**, *52*, 335-338.
- [2] J. Liu, C. Fasel, P. Braga-Groszewicz, N. Rothermel, A. S. Lilly Thankamony, G. Sauer, Y. Xu, T. Gutmann, G. Buntkowsky, *Catalysis Science & Technology* **2016**, *6*, 7830-7840.
- [3] aH. J. Mathieu, *Auger Electron Spectroscopy*, John Wiley & Sons, Ltd, **2009**; bA. D. Hamer, D. G. Tisley, R. A. Walton, *Journal of the Chemical Society, Dalton Transactions* **1973**, 116-120; cA. M. Dennis, R. A. Howard, K. M. Kadish, J. L. Bear, J. Brace, N. Winograd, *Inorganica Chimica Acta* **1980**, *44*, L139-L141; dP. R. Bontcev, M. Miteva, E. Zhecheva, D. Mechandjiev, G. Pneumatikakis, C. Angelopoulos, *Inorganica Chimica Acta* **1988**, *152*, 107-110; eN. F. Gol'dshleger, B. I. Azbel, Y. I. Isakov, E. S. Shpiro, K. M. Minachev, *Journal of Molecular Catalysis A: Chemical* **1996**, *106*, 159-168.
- [4] J. Liu, P. B. Groszewicz, Q. Wen, A. S. L. Thankamony, B. Zhang, U. Kunz, G. Sauer, Y. Xu, T. Gutmann, G. Buntkowsky, *The Journal of Physical Chemistry C* **2017**, *121*, 17409-17416.